# Supplementary Information

# Combination of float charging and occasional discharging to cause serious LIB degradation analyzed by operando neutron diffraction

Tetsuya Omiya[1], Atsunori Ikezawa[1], Keita Takahashi[2], Keiichi Saito[2], Masao Yonemura[3], Takashi Saito[3], Takashi Kamiyama[3], Hajime Arai[1]

[1] Tokyo Institute of Technology 4259, Nagatsuta, Yokohama, Midori-ku, Kanagawa, 226-0026, Japan
[2] NTT Anode Energy Corporation., Granparktower, 3-4-1 Shibaura, Minato-ku, Tokyo, 105-0023, Japan
[3] High Energy Accelerator Research Organization 203-1, Oazashirane, Tokai, Naka, Ibaraki, 319-1195, Japan

**Table S1.** Overview of durability test conditions and parameters.

| Mode | Step | | Parameters | Termination |
|---|---|---|---|---|
| Cycling | 1) | CC Charge | $I$ = 1.675 A (0.5C) | $V$ = 4.2 V |
| | 2) | Charge Rest (OCV) | OCV | $t$ > 10 min |
| | 3) | CC Discharge | $I$ = –3.35 A (1C) | $V$ = 2.5 V |
| | 4) | Discharge Rest (OCV) | OCV | $t$ > 10 min |
| Floating | 1) | CCCV Charge | $I$ = 1.675 A (0.5C), $V$ = 4.2 V | ———— |
| Floating-cycling | 1) | CCCV Charge | $I$ = 1.675 A (0.5C), $V$ = 4.2 V | $t$ > 18 h |
| | 2) | CC Discharge | $I$ = –3.35 A (1C) | $V$ = 2.5 V |
| | 3) | Discharge Rest (OCV) | OCV | $t$ > 5 h |

(a)

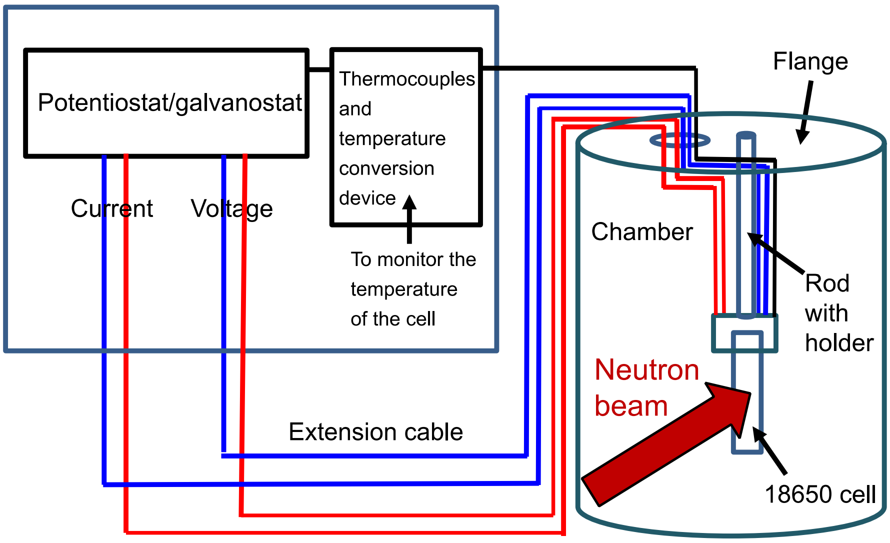


(b)

**Fig.S1** (a) Schematic image of instrumental setup and (b) photo of operando cell in the chamber.

**Table S2.** Discharge capacity values of durability test cell.

| Mode | Tested days or cycle number | Fresh cell capacity [Ah] | After test capacity [Ah] | Relative capacity [%] |
|---|---|---|---|---|
| Cycling | 397 | 2.83 | 2.69 | 95.2 |
| Floating | 397 | 2.84 | 2.74 | 96.4 |
| Floating-cycling | 397 | 2.84 | 2.21 | 77.9 |
| Floating-cycling (0.3C) | 397 | 2.84 | 2.16 | 75.8 |

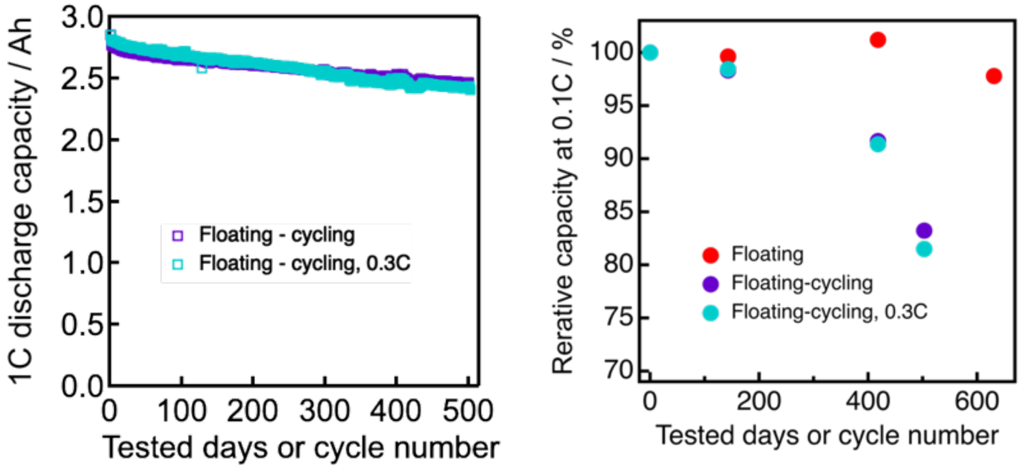


**Fig. S2** Trends of (left) 1C discharge capacity of horizontally-set cells as function of tested days (Floating and Floating-cycling) and (right) the corresponding capacity retention at 0.1C before and after durability test.

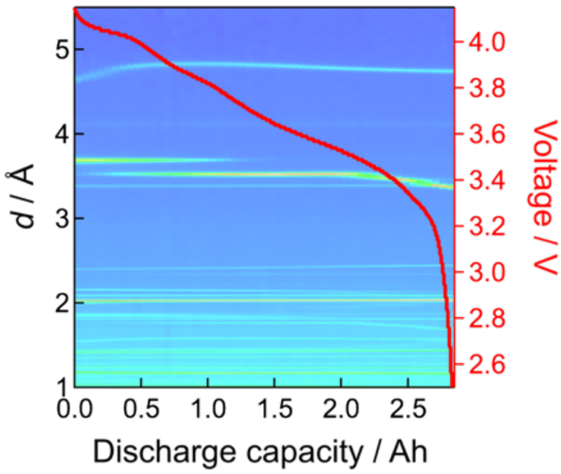


**Fig. S3** Neutron diffraction patterns of the fresh cell. The reflection corresponding to stage 4 of graphite was observed only for the fresh cell, that also appears in the literature[1], suggesting that this is one of a stable phase among lithiated-graphite compounds.

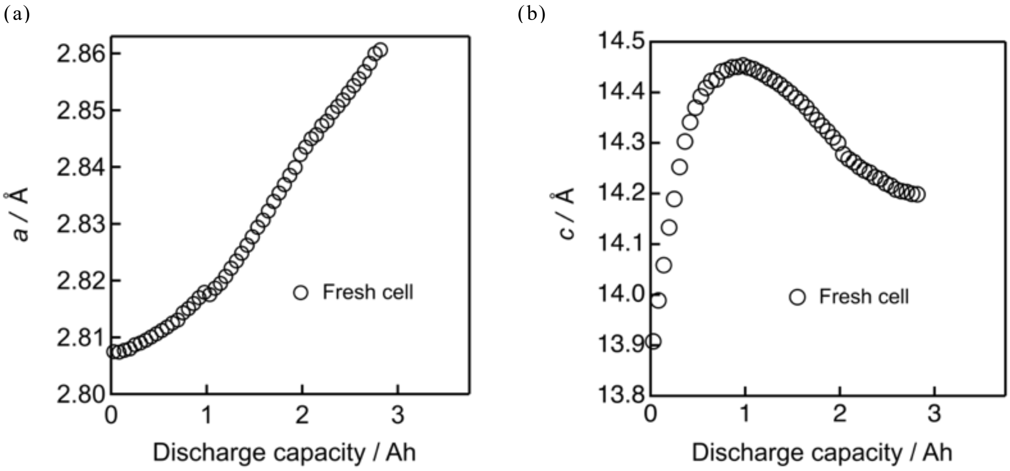


**Fig.S4** Lattice constant evolution of the positive electrode material (a) *a* and (b) *c* for the fresh cell.

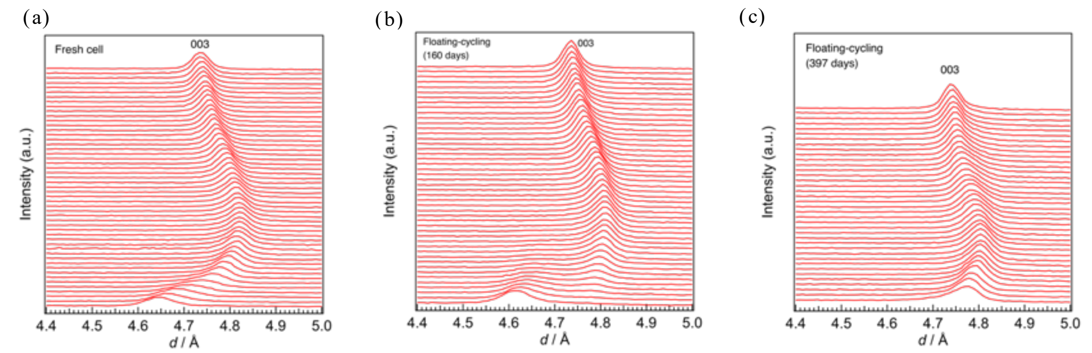


**Fig. S5** The diffraction profiles of the positive electrode 003 reflection of the Floating-cycling cell: (a) Fresh cell, (b) after 160 days, (c) after 397 days.

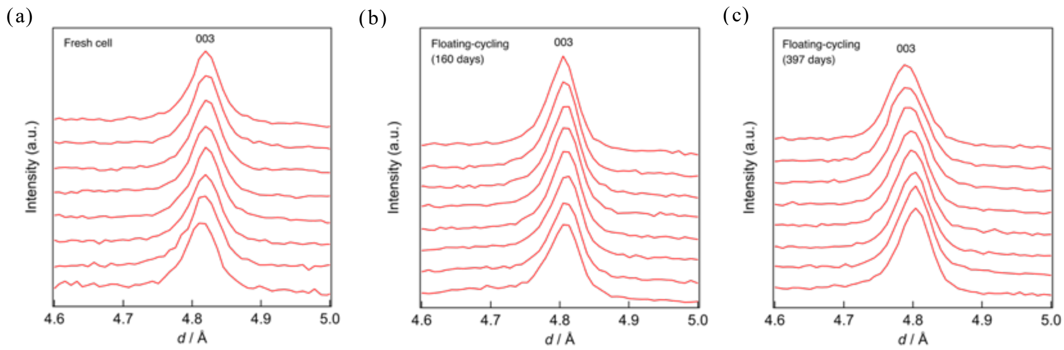


**Fig. S6** The selected diffraction profiles of the positive electrode 003 reflection of the Floating-cycling cell: (a) Fresh cell, (b) after 160 days, (c) after 397 days.

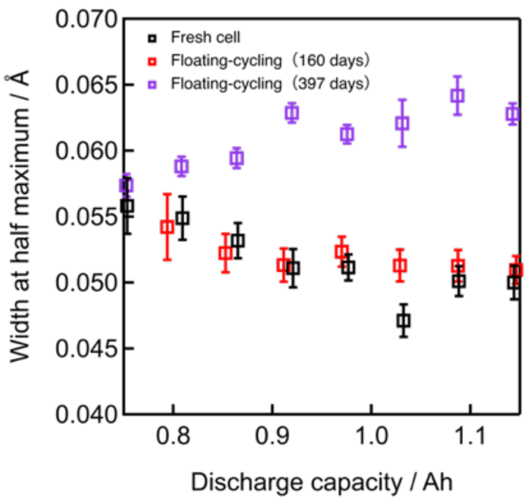


**Fig. S7** The width at half maximum of the diffraction peaks shown in Fig. S5, obtained by Gaussian distribution fitting.

(a)

(b)

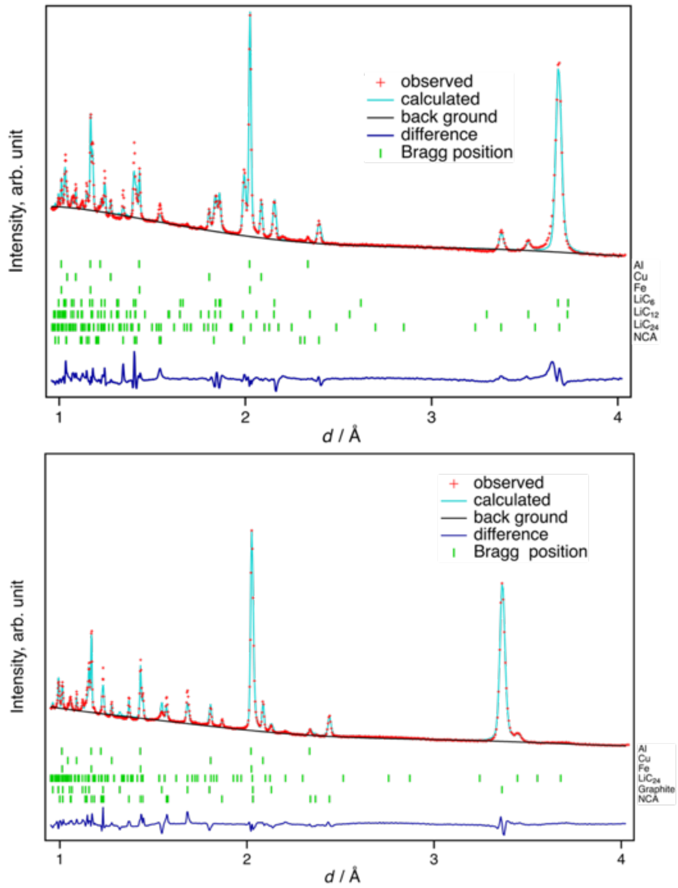


**Fig. S8** Neutron diffraction patterns and results of Rietveld refinement of the fresh cell in (a) fully charged (b) fully discharged states. The background of diffraction patterns is somewhat large, due to the presence of hydrogen atoms in the electrolyte and separator, but it is monotonous and not too significant to interfere the Rietveld analysis as shown in the figure.

(a)

(b)

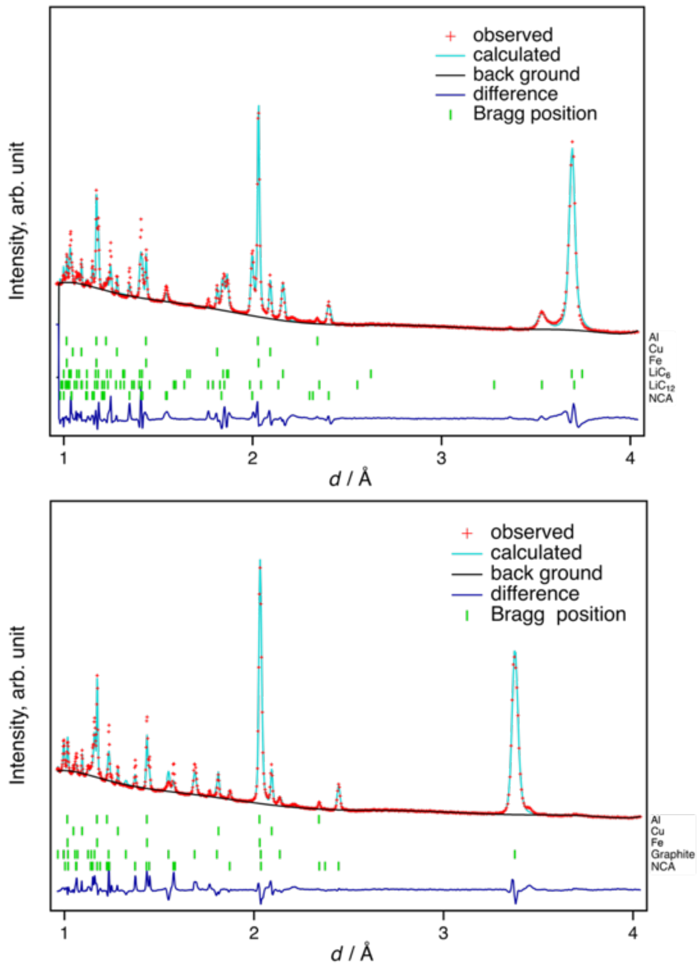


**Fig. S9** Neutron diffraction patterns and results of Rietveld refinement after floating test in (a) fully charged (b) fully discharged states.

(a)

(b)

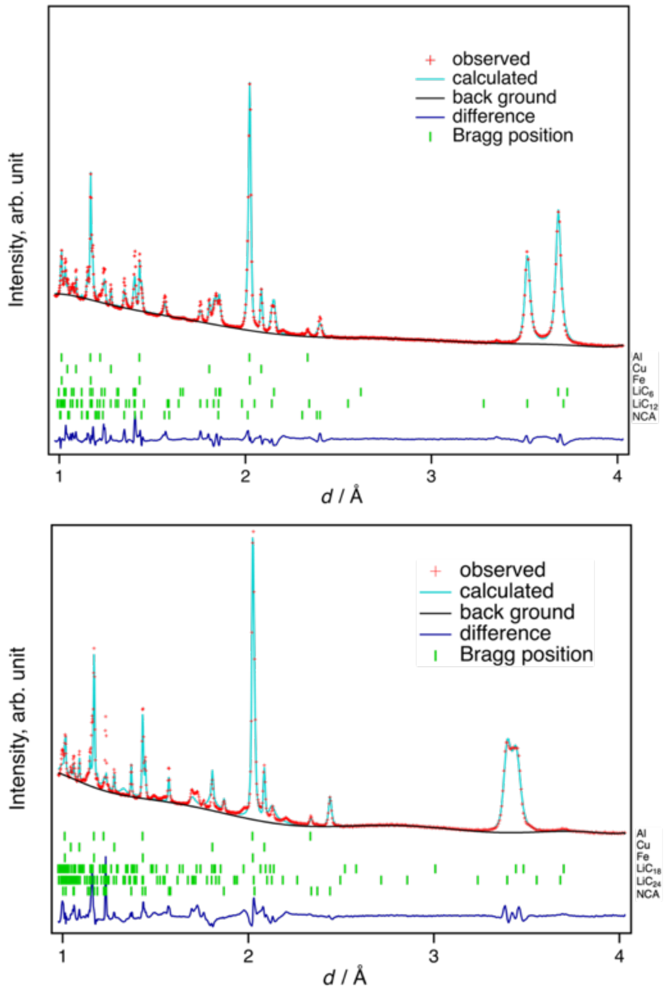


**Fig. S10** Neutron diffraction patterns and results of Rietveld refinement after floating-cycling test in (a) fully charged (b) fully discharged states.

**Table S3.** *R* factors obtained by Rietveld refinement before and after durability tests.

| Mode | State | $S$ | $R_{wp}$ [%] | $R_p$ [%] | $R_e$ [%] |
|---|---|---|---|---|---|
| Fresh cell | Full charged | 8.26 | 4.20 | 2.91 | 0.509 |
| | Full discharged | 8.40 | 4.04 | 2.94 | 0.482 |
| Floating | Full charged | 11.6 | 3.56 | 2.74 | 0.308 |
| | Full discharged | 9.04 | 3.28 | 2.47 | 0.363 |
| Floating-cycling | Full charged | 9.15 | 2.79 | 2.13 | 0.305 |
| | Full discharged | 9.49 | 4.02 | 3.17 | 0.424 |

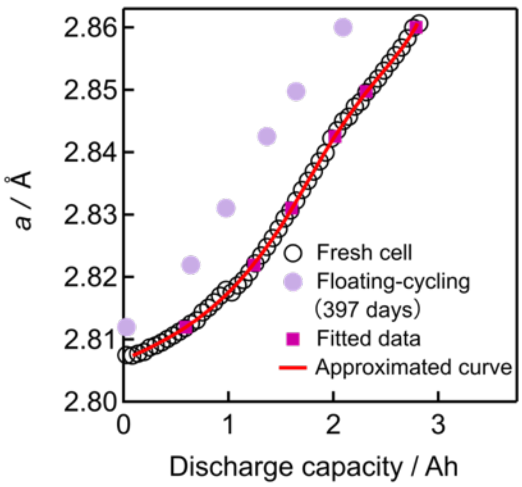


**Fig.S11** The evolution of the positive lattice constant *a* of the Fresh cell during discharging, approximated by the following 6th order function; $y = 2.8075 - 2.9340 \times 10^{-6}x + 3.9646 \times 10^{-8}x^2 - 5.8252 \times 10^{-11}x^3 + 4.4545 \times 10^{-14}x^4 - 1.5851 \times 10^{-17}x^5 + 1.9993 \times 10^{-21}x^6$ , where $x$ is the discharge capacity [mAh] and $y$ is the value of the lattice constant *a* [Å], together with the constants *a* of the Floating-cycling cell during discharging (violet circles). Two parameters, the capacity shift caused by incomplete charging and the expansion rate derived from the loss of the positive electrode active material (due to degradation) were optimized to minimize the root-mean-square errors with the approximation curve. The resultant fitted constants *a* are also shown as pink squares.

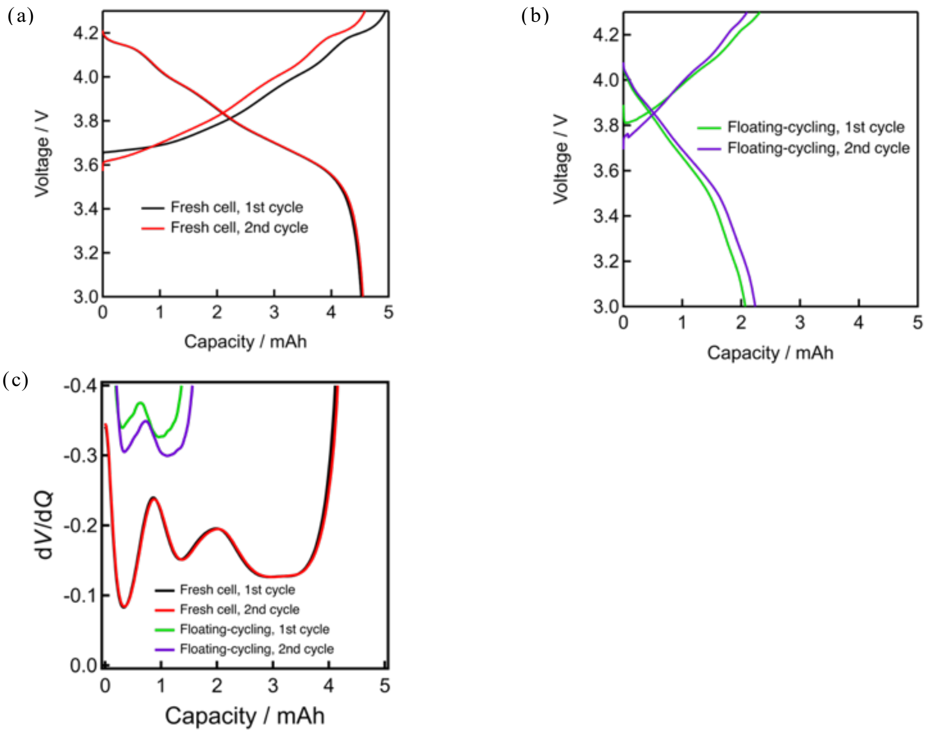


**Fig. S12** Charge-discharge curves and d*V*/d*Q* curves of the positive electrode half cells at the 1st and 2nd cycle: (a) charge-discharge curves of fresh cell, (b) charge-discharge curves of the cell after the Floating-cycling test, (c) corresponding d*V*/d*Q* curves. All half cells have been stored in the fully discharged states for more than two years after full cell disassembling and reassembling to half-cells.

(a) (b)

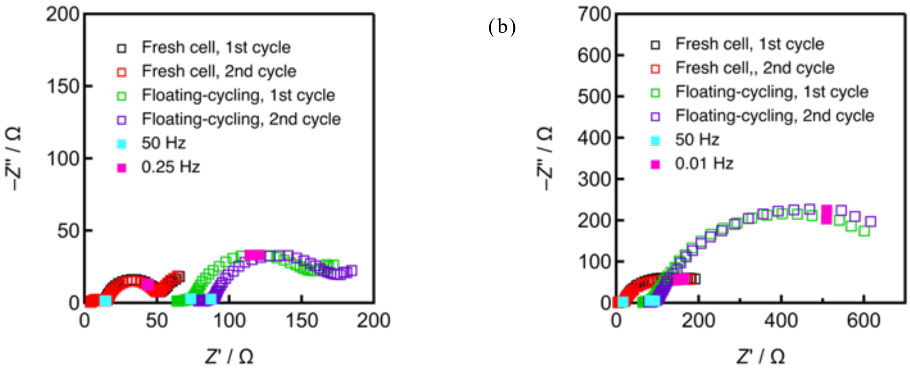


**Fig. S13** Nyquist plots of the positive electrode half cells in (a) fully charged and (b) fully discharged states. All half cells have been stored in the fully discharged states for more than two years after full cell disassembling and reassembling to half-cells.

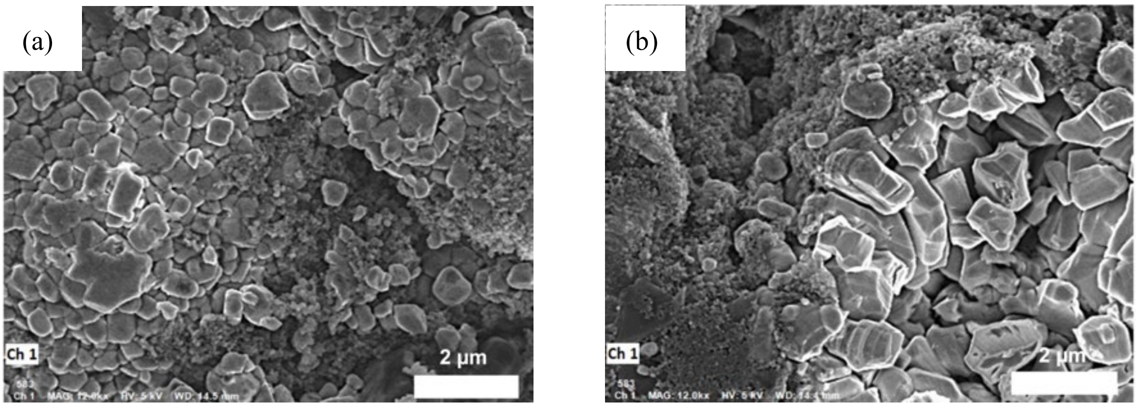


**Fig. S14** SEM images of positive electrode surface: (a) Fresh cell and (b) Floating-cycling.

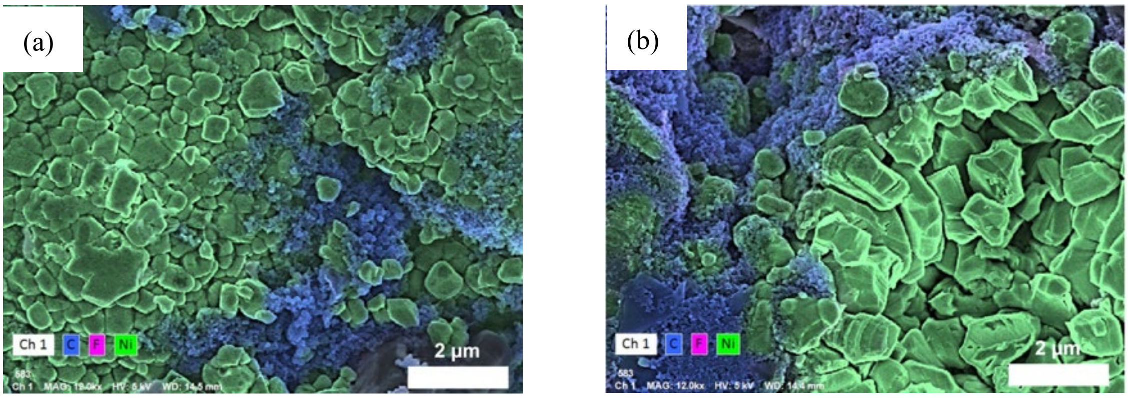


**Fig. S15** EDX results of positive electrode surface: (a) Fresh cell and (b) Floating-cycling.

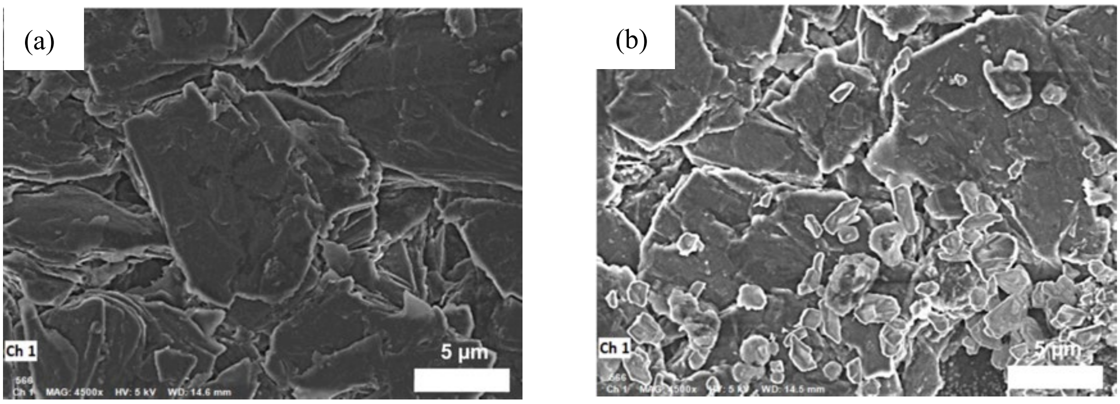


**Fig. S16** SEM images of negative electrode surface: (a) Fresh cell and (b) Floating-cycling.

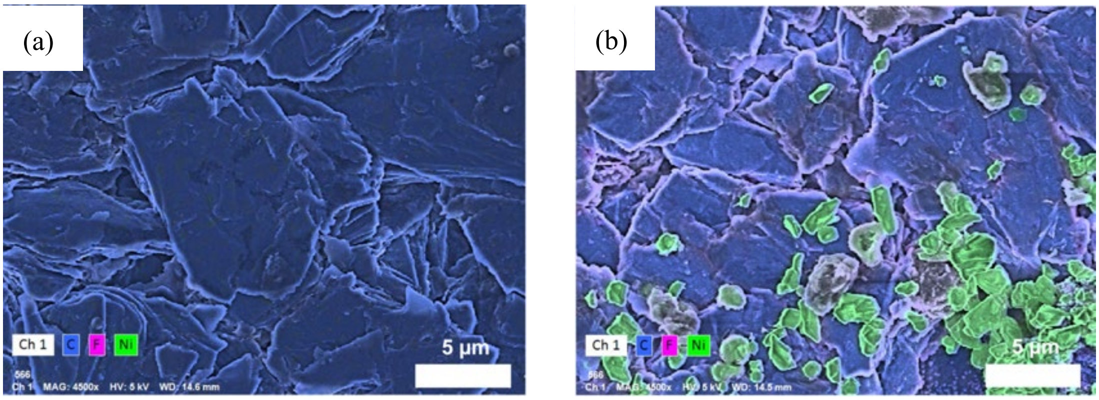


**Fig. S17** EDX results of negative electrode surface: (a) Fresh cell and (b) Floating-cycling.

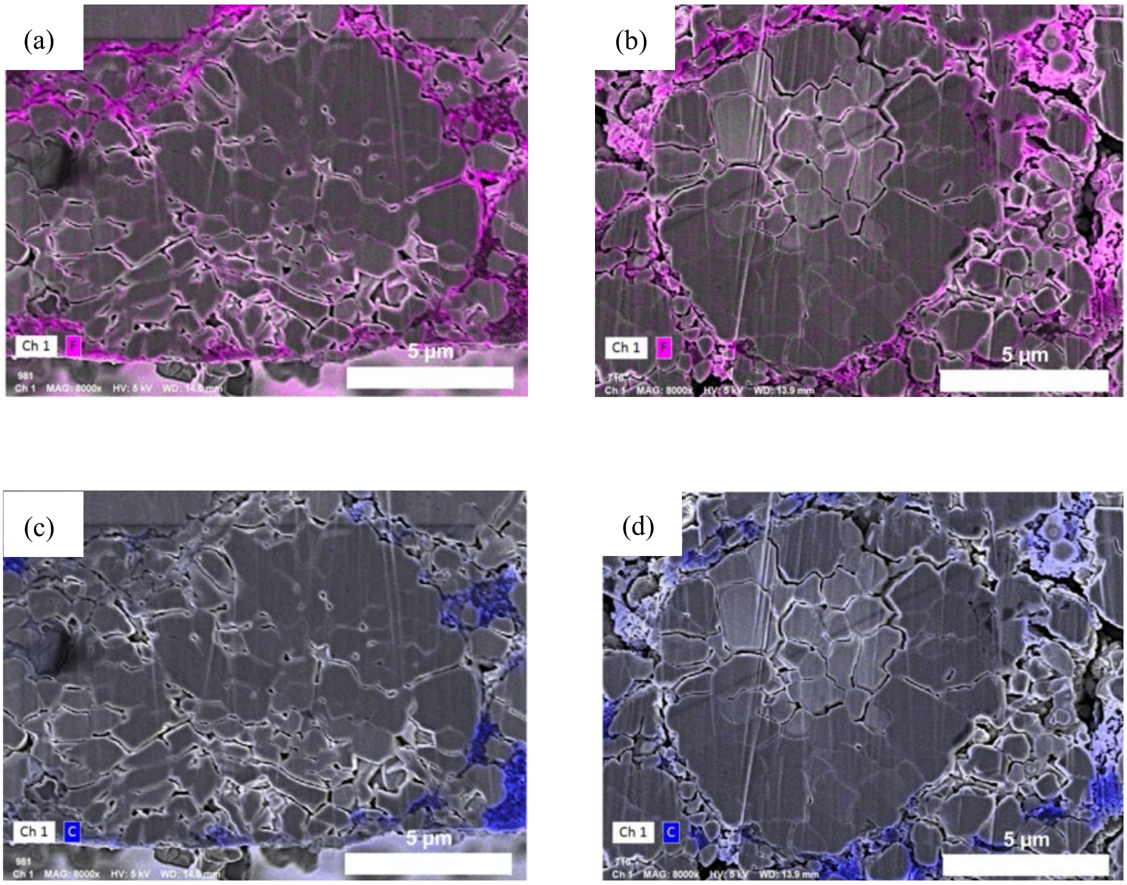


**Fig. S18** EDX results of positive electrode cross section after Floating-cycling test: (a) and (b) fluorine mapping, (c) and (d) carbon mapping, (a) and (c) electrolyte side, (b) and (d) current collector side.

(a)

(b)

(c)

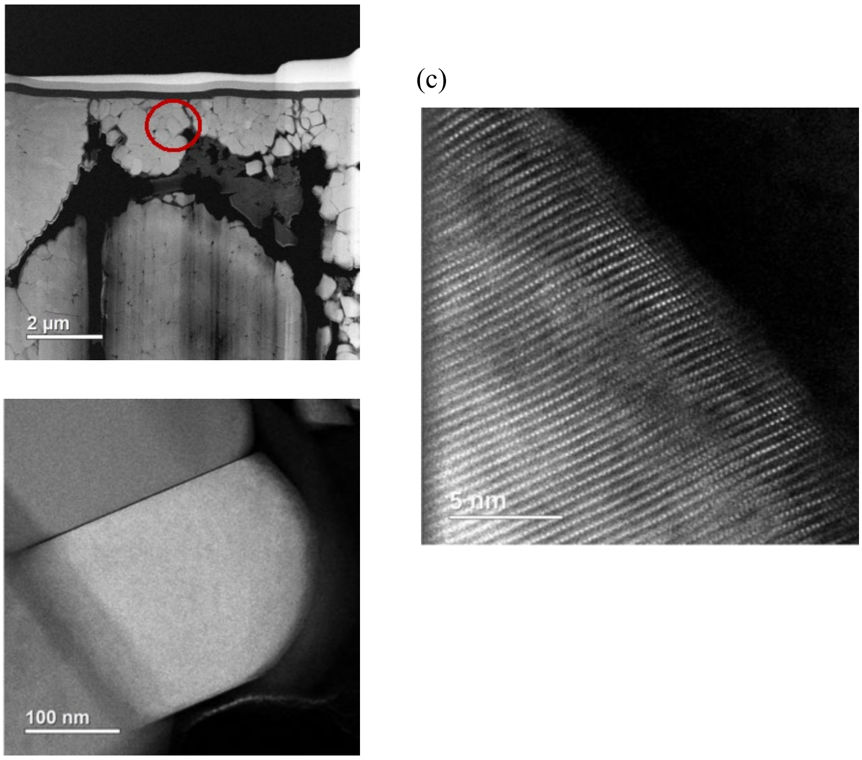


**Fig. S19** Cross-sectional TEM images of the positive electrode particle in the fresh cell (a) Overview of TEM image, (b) Particle TEM image of the marked region in (a), (c) High-magnification TEM image in (b).

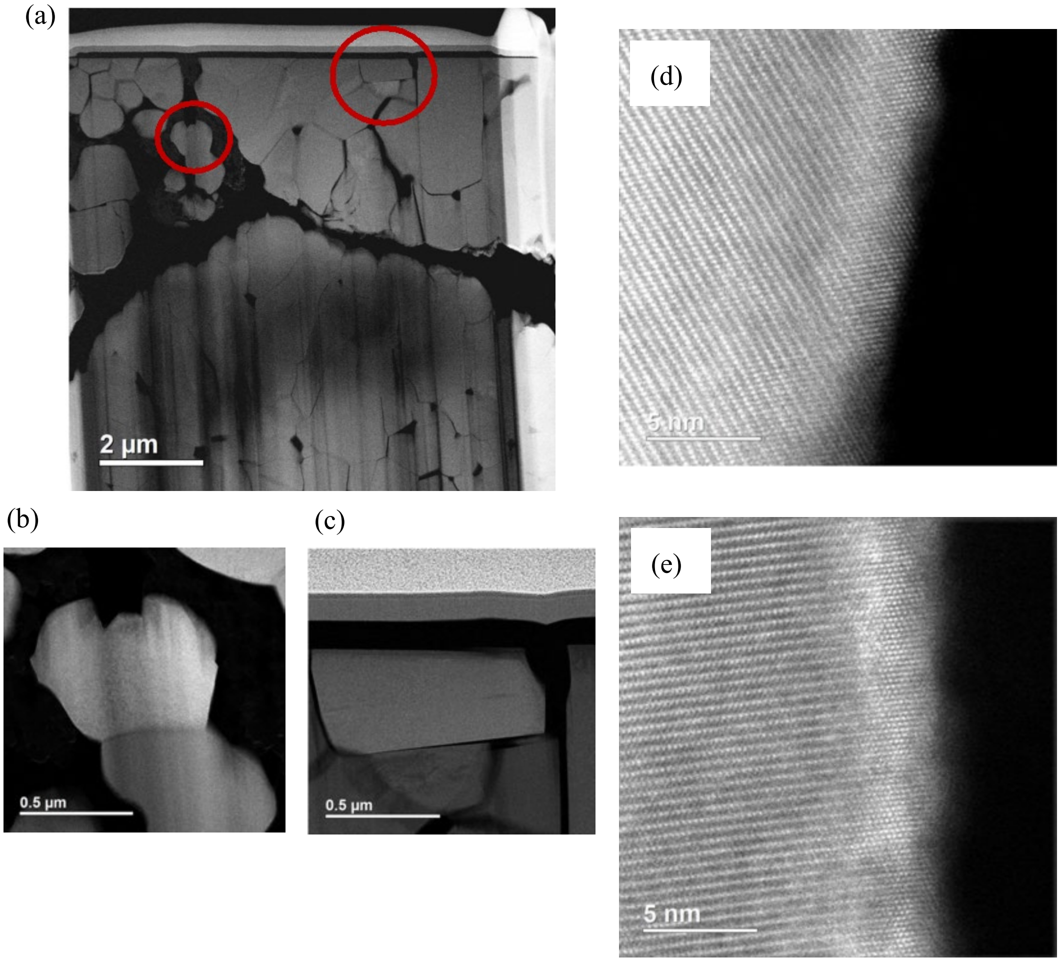


**Fig. S20** Cross-sectional TEM images of the positive electrode in the cell after 397 days of Floating-cycling: (a) Overview of TEM image, (b) Particle TEM image of the active material surface, (c) particle image in the crack region, (d) High-magnification TEM image in (b), (e) High-magnification TEM image in (c).

## Reference

1. L. B. Roblin, D. Sheptyakov, P. Borel, C. Tessier, P. Novák, and C. Villevieille, Crystal structure evolution via operando neutron diffraction during long-term cycling of a customized 5 V full Li-ion cylindrical cell $LiNi_{0.5}Mn_{1.5}O_4$ *vs*. graphite, *J. Mater. Chem. A*, 2017, **5**, 25574–25582, doi: 10.1039/c7ta07917f.